

# Dipolar Dislocation Walls: Origin, Role and Formulation in Discrete/Continuum Multiscale Dislocation Dynamics

PI and SP

(Dated: January 27, 2017)

1. present

Crystals primarily deform through the motion of dislocations. This sole fact can provide key explanations for the magnitude and character of uniaxial and shear strength, as well as the plastic crystalline behavior. While this is an undeniable fact, it has been relatively unknown whether the patterns that such dislocation ensembles may form, as they move, can influence the magnitude and/or character of crystalline mechanical strength and plastic behavior. It has been postulated that the transition between Stage II and Stage III hardening regimes in metals is associated to dislocation patterning, grain-boundary formation and dislocation cell walls (see for example, Refs. [1]), [2], [3]. [4][5][6][7].

It has been also observed that yielding due to mechanical fatigue is preceded by the formation of complex dislocation patterns that have been labeled as “vein structures”, typically observed in TEM after multiple thousands of fatigue cycles [8], [9], [10]. Such vein structures have been postulated to be dominated by dipolar dislocation walls, namely the formation of aligned structures of many opposite-signed dislocations which strongly attract but may not annihilate, since they are located in nearby but different slip-planes. Such dipolar dislocation walls have been observed in TEM studies of fatigued metals, but their dynamic origin is as much unknown as the origin of the vein structures. However, as soon as they emerge, it is clear that their highly stable character (due to the very strong, attractive dislocation-dislocation interactions) would hinder further homogeneous motion of dislocations and eventually lead to strain-localization through the formation of persistent slip bands (PSB). [11], [12]. The way with which such a remarkable transition sequence (homogeneous plasticity to dipolar walls and vein structures to PSBs) takes place during persistent fatigue remains unknown. While this is a clear example of emergent patterning in a non-equilibrium setting, and therefore interesting to understand and correlate with other analogous statistical phenomena, it is also vital to characterize such patterns in order to predict the number of cycles required for mechanical failure.

Dipolar dislocation walls have been naturally observed in an explicit example of mechanical deformation: that of monotonically increasing shear of 2D discrete edge dislocation dynamics in an initially random dislocation ensemble. Such walls have been observed to be emergent at high strains, beyond  $\epsilon_c$  % strain, and also at quite large overall net dislocation densities. The mechanical stability of such walls is so high that no dislocation can further cross through in this system. [13][14][15].

While the emergence of dipolar dislocation walls has

been observed in a special example of 2D discrete dislocation dynamics simulations, their dynamical origin has not been clear. It has been postulated that their origin is associated with the contribution of backstress terms in continuum dislocation dynamics: Backstress terms are typically associated with asymmetric tension/compression behavior in crystal plasticity [16], and effects such as the Bauschinger effect, and they represent the key ingredients in theories of kinematic hardening. [17], [18] In dislocation dynamics, such terms are naturally connected to any dynamical terms in the equation of motion (for dislocation densities) that are not locally proportional to the density – then asymmetries are expected to emerge. [14], [19]. While there are several theories of kinematic hardening, the functional form of backstress, as well as overall signs of fitting coefficients, are regarded as material parameters, independent of the basic behavior of the system. Furthermore, no connection of such parameters and their signs has been identified with emergent crystal plastic behaviors, such as dipolar dislocation walls.

In this paper, we elucidate the origin of such dipolar walls in the context of a precise continuum counterpart of dislocation dynamics. We develop a stochastic continuum framework, in which such walls emerge in a direct correspondence with the discrete ones, and we further establish basic constitutive rules for having such emergent walls in continuum dislocation plasticity theories. The key ingredient is a particular form of a backstress term in the continuum dislocation dynamics that contains a dimensionless prefactor. We show that dipolar wall formation only occurs if this parameter falls in a certain range. Our results, therefore, shed new light on the origin of the backstress as well as its role in dislocation patterning of bulk single crystals, and provide a successful multi-scale description of the dynamics.

Modeling the evolution of discrete dislocations in a medium [called discrete dislocation dynamics (DDD)] has become a state-of-the art methodology in the last few decades both in 2D [ ] and 3D [ ]. Whereas the first class considers a model system that is a strong simplification of a realistic network of curved dislocations, advantages of 2D models lie in their superior speed and accuracy that allows studying larger ensembles and/or strains, while still preserving the basic physics of dislocations. On the other hand, a higher scale model describing the evolution of continuous dislocation density fields that is derived from microscopic considerations using a rigorous coarse graining procedure currently only exists for 2D single slip configurations [ ], although significant steps have

TABLE I. Summary of the units of dimensionless quantities.

Quantity	Unit
Distance ( $x$ )	$\rho_0^{-1/2}$
Stress ( $\tau$ )	$Gb\rho_0^{1/2}$
Strain ( $\gamma$ )	$b\rho_0^{1/2}$
Time ( $t$ )	$MGb^2\rho_0$
Dislocation density ( $\rho, \kappa$ )	$\rho_0$

been made in 3D, too [1]. In addition, a proper description of patterning and its physical origin is still lacking even in the relatively simple 2D models. So, before engaging in understanding complex 3D patterning phenomena in the present paper we restrict ourselves to 2D problems.

We consider, therefore, a configuration of straight parallel edge dislocations in single slip. This system is effectively 2D and we track the motion of dislocations in the  $z = 0$  plane. To mimic an infinite crystalline medium periodic boundary conditions (PBC) are applied at the borders of the square shaped simulation area of size  $L \times L$ . The  $x$  axis is chosen to be parallel both with the dislocation slip direction and one of the edges of the simulation cell. In this case the Burgers vector of the dislocations can be written as  $\mathbf{b}_i = s_i \mathbf{b}$ , where  $\mathbf{b} = (b, 0)$ ,  $b$  is the magnitude of the Burgers vector,  $s_i = \pm 1$ , and  $1 \leq i \leq N$ , with  $N$  being the total number of dislocations. We prescribe that the system is neutral ( $\sum_{i=1}^N s_i = 0$ ) and denote the position of the dislocations as  $\mathbf{r}_i = (x_i, y_i)$ . Dislocation motion is assumed to be overdamped, so equation of motion of discrete dislocations can be written as:

$$\dot{x}_i(t) = s_i \left[ \tau_{\text{ext}} + \sum_{j=1, j \neq i}^N s_j \tau_{\text{ind}}(\mathbf{r}_i - \mathbf{r}_j) \right]; \quad \dot{y}_i(t) = 0, \quad (1)$$

where  $\tau_{\text{ind}}$  denotes the stress field of an individual positive ( $s_i = +1$ ) dislocation (the double sum accounts for the periodic images introduced by the PBC):

$$\tau_{\text{ind}}(\mathbf{r}) = \sum_{i,j=-\infty}^{\infty} \frac{(x - iL)[(x - iL)^2 - (y - jL)^2]}{[(x - iL)^2 + (y - jL)^2]^2}, \quad (2)$$

and  $\tau_{\text{ext}}$  is an external load. Here and in the rest of this paper dimensionless units are used by normalizing quantities with the units summarized in Table I. In the definitions  $\rho_0$  stands for the average dislocation density in the system,  $G = \mu/[2\pi(1 - \nu)]$  is an elastic constant containing the shear modulus  $\mu$  and the Poisson ratio  $\nu$ , and  $M$  is the dislocation mobility.

The discrete simulations are started from a random (thus non-equilibrium) configuration of dislocations. First, a relaxation step is performed, that is, Eq. (1) is solved for each dislocation at zero applied stress, then  $\tau_{\text{ext}}$  is increased in a quasistatic manner, allowing relaxation at constant stress every time a strain avalanche sets on (for details see [1]). The typical evolution of the configuration can be seen in the left column of Fig. 1(a). At zero

stress specific local (low energy) configurations can be observed: Opposite sign dislocations organize into short dipoles whereas those of identical sign form short vertical walls. As the applied stress increases the distribution becomes increasingly heterogeneous with the dominance of long dense vertical walls. A closer look to these walls reveals their asymmetric dipolar nature induced by the positive external stress: Positive dislocations tend to be found on the left side, while negative dislocations populate the right side of the walls. Just before yielding configurations typically consist of a single straight merged dipolar wall. One concludes that this is the strongest configuration that can be formed in this 2D system. The stress-strain curve corresponding to this process is seen in Fig. 1(b). For a detailed analysis of its features and size dependence the reader is referred to Refs. [1].

We now continue with introducing the continuum theory that aims modeling the DDD simulations described above. We start from the theory of Groma and co-workers that has been derived from Eq. (1) using a rigorous coarse graining procedure [2]. The recently revisited form of the evolution equations that govern the evolution of continuous density fields  $\rho_{\pm}(\mathbf{r}, t)$  are as follows:

$$\partial_t \rho_+ = -\partial_x \left\{ \rho_+ \left[ \tau_{\text{ext}} + \tau_{\text{sc}} + \tau_b - 2 \frac{\rho_-}{\rho} \tau_f + \tau_d \right] \right\}, \quad (3)$$

$$\partial_t \rho_- = +\partial_x \left\{ \rho_- \left[ \tau_{\text{ext}} + \tau_{\text{sc}} + \tau_b - 2 \frac{\rho_+}{\rho} \tau_f - \tau_d \right] \right\}, \quad (4)$$

where

$$\tau_{\text{sc}}(\mathbf{r}, t) = \int \tau_{\text{ind}}(\mathbf{r} - \mathbf{r}') \kappa(\mathbf{r}', t) d^2 r', \quad (5)$$

$$\tau_b(\mathbf{r}, t) = -\frac{D}{\rho} \partial_x \kappa(\mathbf{r}, t), \quad (6)$$

$$\tau_d(\mathbf{r}, t) = -\frac{A}{\rho} \partial_x \rho(\mathbf{r}, t), \quad (7)$$

and  $\tau_f$  is the ‘flow stress’ that is, in accordance with the Taylor relationship, assumed to be  $\alpha \rho^{1/2}$ . Here we used notations  $\rho = \rho_+ + \rho_-$  for the total and  $\kappa = \rho_+ - \rho_-$  for the geometrically necessary dislocation (GND) density, while  $D$  and  $A$  are dimensionless constants. (We recall the the equations are written using the dimensionless variables introduced above.)

In Eqs. (3,4) the self-consistent field  $\tau_{\text{sc}}$  is the long-range stress field of GNDs which together with the external field  $\tau_{\text{ext}}$  represents an experimentally measurable quantity: The average shear stress in a small volume around  $\mathbf{r}$ . These stress terms are complemented by the flow stress  $\tau_f$  and local gradient terms  $\tau_b$  (back-stress) and  $\tau_d$  (diffusion stress). The origin of these latter terms is clear from the formal derivation of the theory [2]: They stem from the fact that dislocations are not positioned randomly but are spatially correlated, a fact that has been already postulated by Wilkens based on energetic considerations [3] and also proved by numerical simulations [4]. Dislocation patterns themselves are also a man-

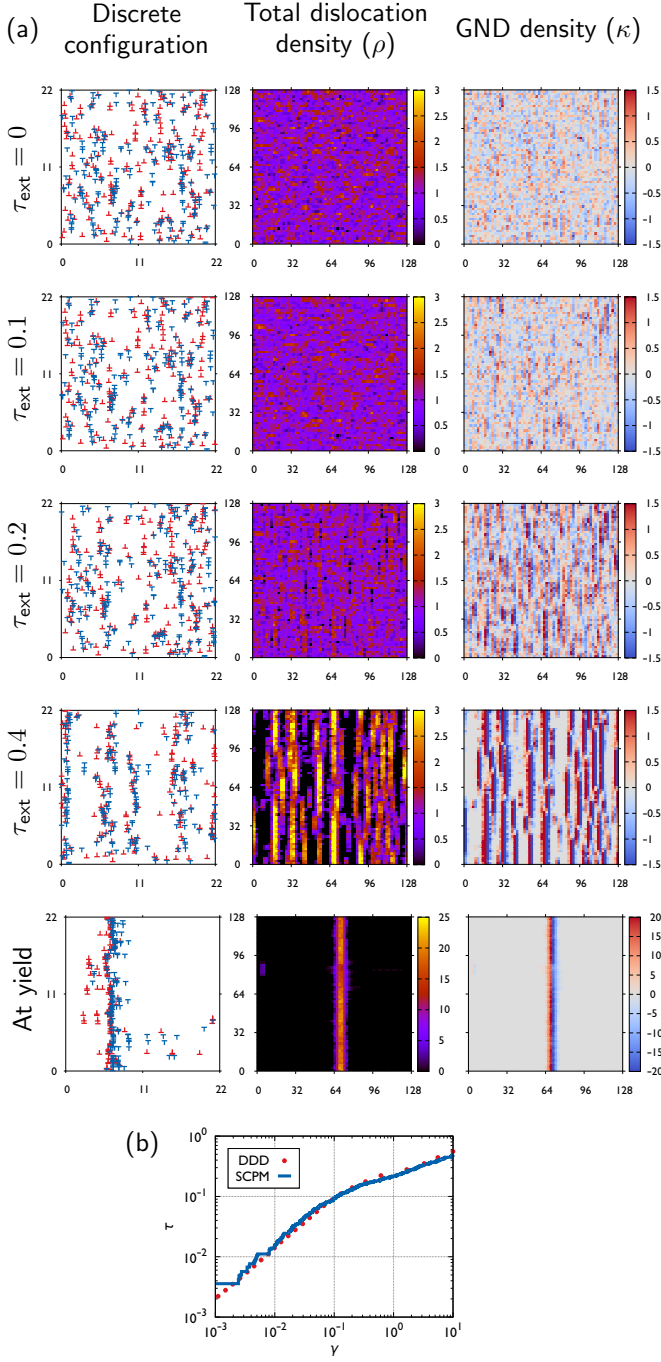


FIG. 1. Comparison of dislocation pattern evolution and plastic response for DDD and SCCP simulations. In the case of SCCP the following simulation parameters were used:  $a = 2$ ,  $D = -0.6$ ,  $A = 0.6$ , and  $Y = 1.0$ . (a,b,c): Dislocation configurations obtained by DDD (left column) and density maps from SCCP simulations (total and GND densities in the middle and right columns, respectively). The rows correspond to different strains: (a)  $\gamma = 0$  (b) intermediate ( $\gamma = 0.7$  for DDD and  $\gamma = 10$  for SCCP) and (c) at the onset of final yield. Note that due to the PBC the actual position of the emerging vertical wall does not bear any physical relevance. (d): Average stress-strain curves for the two types of simulations.

ification of these correlations. As of the physical meaning of these terms, flow stress is the result of the small-scale correlated substructures (most importantly, dislocation dipoles) discussed above that may be stable against external load. Indeed, in Eqs. (3,4)  $\tau_f$  is multiplied by  $\rho_{\pm}$  expressing that dislocations can only be withheld by dislocations of opposite sign. Interpretation of gradient terms are more subtle: They can be envisaged as a correction to the flow stress. In particular, due to the back-stress term local strength may depend on the gradient of the GND density as depicted in the sketch of Figure 2. According to the sign of parameter  $D$  the strength of the local volume (or region of interest, ROI) in Fig. 2(b) may be larger ( $D < 0$ ) or smaller ( $D > 0$ ) than that of Fig. 2(a). Similar explanation can be given for the diffusion stress  $\tau_d$ , too.

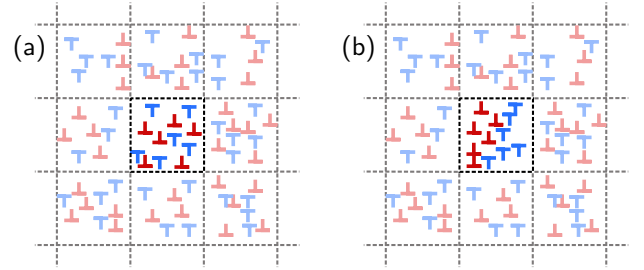


FIG. 2. A gradient in the GND density is one form of spatial correlations that may affect local strength (through the back-stress  $\tau_b$ ) and lead to different yielding thresholds for panels (a) and (b). Configuration of panel (b) is stronger (weaker) if  $D < 0$  ( $D > 0$ ). The dashed lines denote spatial discretization which is necessary to define continuous densities.

The continuum theory does not yield exact values for the parameters  $D$  and  $A$ , one must, therefore, consider them as fitting parameters. The results of DDD simulations summarized above, however, give a strict constraint on possible values. As seen in Fig. 1(a) the strongest possible dislocation configuration is the dipolar wall structure. According to Fig. 2 this implies the necessity of the back-stress term  $\tau_b$  and that  $D < 0$ .

The numerical implementation of Eqs. (3,4) is based on the method of Zaiser and Moretti [1]: Densities are discretized on a regular grid of cell size  $a$ , and the flow stress  $\tau_f$  is replaced by a local stochastic variable (representing the fluctuations of the underlying dislocation microstructure at every cell). For the distribution of the yield stress a Weibull distribution is used with shape parameter 1.4 and scale parameter  $Y$  [1]. In addition, we use extremal dynamics: As long as the local stress is below the yielding threshold in a given cell (e.g.,  $\tau_{\text{ext}} + \tau_{\text{sc}} < 2(\rho_-/\rho)\tau_f - \tau_b - \tau_d$  for + dislocations) no activity happens, otherwise a quantum of dislocation flux  $\Delta\rho = a^{-2}$  (of either positive or negative dislocations) flows through a cell boundary. Further details of the implementation are summarized in the Supplementary Material. In the rest of this Letter we will refer to this model as stochastic crystal plasticity (SCCP).

In accordance with the DDD case simulations are started from a random pattern of  $\rho_+$  and  $\rho_-$  and initially a relaxation step is performed at  $\tau_{\text{ext}} = 0$ . Then the external stress  $\tau_{\text{ext}}$  is gradually increased leading to the evolution of the dislocation densities. The center and right column of Fig. 1(a) depicts this evolution for a given parameter set ( $D = -0.6$ ,  $A = 0.8$ ,  $Y = 1.0$ ,  $a = 2$ ). As seen a remarkable similarity is obtained between DDD and continuum simulations since dipolar walls form in the latter case, too, as proved by the GND density maps. To quantitatively compare DDD and SCCP results we introduce the spatial cross-correlation of dislocations of opposite sign as

$$C_{+-}(\Delta\mathbf{r}) = \int \rho_+(\mathbf{r})\rho_-(\mathbf{r} + \Delta\mathbf{r})d^2r \quad (8)$$

and consider its average along the  $y$  axes:  $C_{+-}(\Delta x) = \langle C_{+-}(\Delta x, \Delta y) \rangle_{\Delta y}$ . This quantity measures the level of asymmetry, that is, the polarization of the configurations. As seen in the insets of Fig. 3 at zero strain this function is indeed invariant for  $\Delta x \rightarrow -\Delta x$  substitution, and a strong asymmetry emerges upon plastic deformation for both models. We introduce the quantity  $o := \int_0^{L/2} [C_{+-}(\Delta x) - C_{+-}(-\Delta x)]d\Delta x$  as a single measure of the level of internal polarization. According to Fig. 3 this parameter initially increases linearly with strain for both models. At larger strains a difference is seen that can be attributed to the different system sizes of the two models.

Now we turn at addressing the role of the parameters of SCCP in the patterning. Figure 4 plots the dependence of parameter  $o$  on the coefficients of the gradient terms  $D$  and  $A$ . It is clear, that the presence of dipolar walls is not dependent on  $A$  and is conditioned on  $D < -0.5$ . This can be explained by noticing, that in the middle of a “+−” dipolar wall  $\tau_d = 0$  and the sum of  $\tau_{\text{sc}}$  and  $\tau_b$  is negative (positive) if  $D < -0.5$  ( $D > -0.5$ ). The details of the simple derivation are summarized in the Supplementary Material, but we highlight that the result is independent of the choice of  $a$ . One concludes, thus, that the back stress  $\tau_b$  alone is responsible for dipolar wall formation. As of the role of the remaining parameters:  $\tau_d$  is a diffusive term [] so increasing  $A$  leads to the “blurriness” of the dislocation patterns, whereas modifying  $Y$  and  $a$  primarily affect the scale and shape of the stress-strain curves.

It is instructive to compare the continuum plasticity theory with general elastoplastic constitutive models, in particular, with those of kinematic hardening. The back-stress term appearing therein is of completely different origin as it aims at modeling the Bauschinger effect observed at reversed loading with the appropriate translation of the yield surface []. Their practical role, however, are identical, since  $\tau_b$  in Eqs. (3,4) can also be considered as an asymmetric correction to  $\tau_y$ . In addition, using the identity  $\partial_t \kappa(\mathbf{r}, t) = -\partial_x \dot{\gamma}(\mathbf{r}, t)$  connecting the GND density with the shear component  $\gamma$  of the plastic

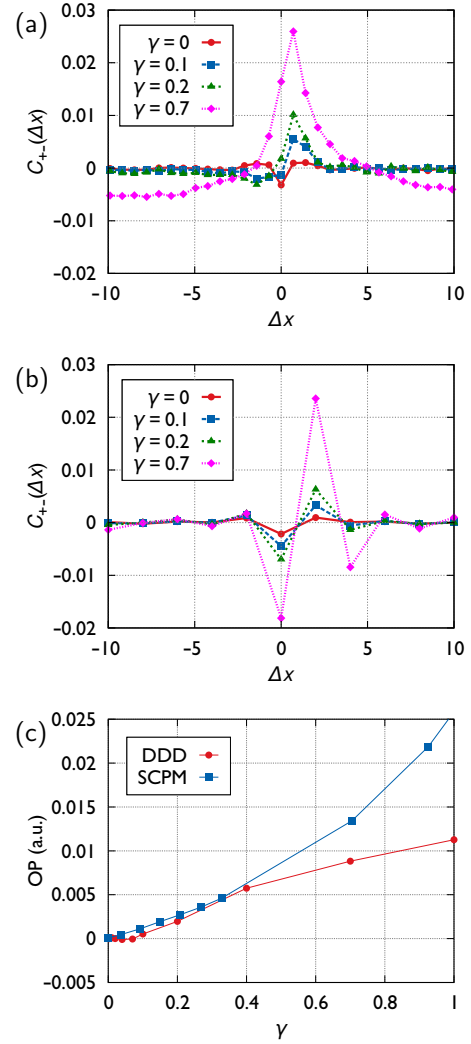


FIG. 3. (a,b):  $C_{+-}$  cross correlation functions for DDD (a) and SCCP (b). Panel (c): the evolution of the order parameter for the two types of simulations. The parameters are the same as in Fig. 1.

strain rate one arrives at  $\dot{\tau}_b = (D/\rho)\partial_x^2 \dot{\gamma}$  that is analogous to the phenomenological rate equation of Melan and Prager ( $\tau_b \propto \dot{\gamma}$ ) [] (the appearance of the second derivative reflects the difference that quantities are global in the constitutive theory and local in the present continuum theory). The simulations presented above, therefore, emphasize the microscopic origin of the back-stress: The asymmetry of the yield surface in kinematic hardening is the result of the build-up of asymmetric dislocation sub-structures (dipolar walls in the present set-up).

Back-stress terms are also used in gradient plasticity theories to account for the short-range interactions in pile-ups close to grain boundaries []. Such terms exhibit the same form as Eq. (6) but with a positive dimensionless prefactor, while we obtained  $D < 0$  here. The difference can be readily explained by noticing that pile-ups mainly consist of GNDs. In such a case, if the

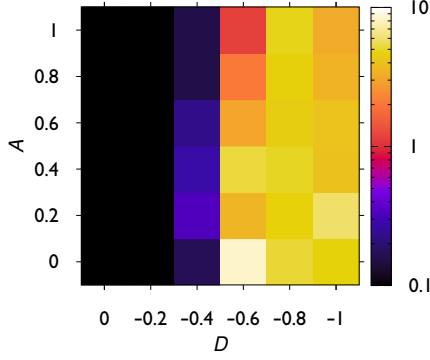


FIG. 4. Phase diagram for  $Y = 1.0$  and  $a = 2$ .

pile-up contains, e.g., + dislocations (that is,  $\kappa = \rho$ ) the flow-stress disappears from Eq. (3) and the two gradient

terms merge into one as  $\tau_b + \tau_d = -(D + A)(1/\rho)\partial_x \kappa$ . This means that in this fully polarized situation, in accordance with the plasticity theories, only one back-stress term remains preceded with a possibly positive prefactor even with  $D < 0$  (like for the particular parameter set obtained above).

TODO:

- noise also scales with  $\sqrt{\rho}$
- fig 4 for  $\gamma = 10$
- recalculate  $o$  with the new definition
- Merge Fig 3 subfigs into one and caption
- citations
- abstract and conclusions
- supplementary material

- 
- [1] Y. S. Chen, W. Choi, S. Papanikolaou, and J. P. Sethna, *Physical review letters* **105**, 105501 (2010).
  - [2] H. Mughrabi, T. Ungar, W. Kienle, and M. Wilkens, *Philosophical magazine A* **53**, 793 (1986).
  - [3] C. Schwink, *Scripta metallurgica et materialia* **27**, 963 (1992).
  - [4] P. Hähner, K. Bay, and M. Zaiser, *Physical review letters* **81**, 2470 (1998).
  - [5] D. Hughes, Q. Liu, D. Chrzan, and N. Hansen, *Acta materialia* **45**, 105 (1997).
  - [6] D. Hughes, D. Chrzan, Q. Liu, and N. Hansen, *Physical review letters* **81**, 4664 (1998).
  - [7] E. Laufer and W. Roberts, *Philosophical Magazine* **14**, 65 (1966).
  - [8] S. Suresh, *Fatigue of materials* (Cambridge university press, 1998), ISBN 0521578477.
  - [9] H. Mughrabi, F. u. Ackermann, and K. Herz, *Persistent slipbands in fatigued face-centered and body-centered cubic metals* (ASTM International, 1979).
  - [10] D. Walgraef and E. C. Aifantis, *Journal of applied physics* **58**, 688 (1985).
  - [11] D. Kuhlmann-Wilsdorf and C. Laird, *Materials Science and Engineering* **46**, 209 (1980).
  - [12] T. Tabata, H. Fujita, M.-A. Hiraoka, and K. Onishi, *Philosophical Magazine A* **47**, 841 (1983).
  - [13] P. D. Ispánovity, I. Groma, G. Györgyi, F. F. Csikor, and D. Weygand, *Physical review letters* **105**, 085503 (2010).
  - [14] I. Groma, F. Csikor, and M. Zaiser, *Acta Materialia* **51**, 1271 (2003).
  - [15] P. D. Ispánovity, L. Laurson, M. Zaiser, I. Groma, S. Zapperi, and M. J. Alava, *Physical review letters* **112**, 235501 (2014).
  - [16] R. Asaro and V. Lubarda, *Mechanics of solids and materials* (Cambridge University Press, 2006), ISBN 1139448994.
  - [17] W. Prager, *Proceedings of the Institution of Mechanical Engineers* **169**, 41 (1955).
  - [18] W. Prager, *J. Applied Mechanics* **23**, 482 (1956).
  - [19] M. Zaiser, N. Nikitas, T. Hochrainer, and E. Aifantis, *Philosophical Magazine* **87**, 1283 (2007).